Electronic Supplementary Material (ESI) for Nanoscale.

Supporting Information

Capacity fading mechanism and improvement of cycling stability in MoS_2-based anode materials for lithium ion Batteries

Haibo Shu [*,a,c] Feng Li,[a] Chenli Hu,[a] Pei Liang,[a] Dan Cao,[b] and Xiaoshuang Chen[c]

[a]College of Optical and Electronic Technology and [b]College of Science, China Jiliang University, 310018 Hangzhou, China

[c] National Laboratory for Infrared Physics, Shanghai Institute of Technical Physics, Chinese Academy of Science, 200083 Shanghai, China

*Corresponding author. Haibo Shu, Phone: +86-0571-86875648, E-mail: shu123hb@gmail.com

I. Models and energetics of Li adsorption/intercalation in MoS_2 nanosheets

The models of single Li ion adsorption and intercalation in MoS_2 nanosheets are shown in Fig. S1 and Fig. S2, respectively. For the Li adsorption on the surface of MoS_2 nanosheet (see Fig. S1), three configurations including hcp hollow (S_1), fcc hollow (S_2), and top (S_3) sites are considered for both 2H and 1T phases. For the Li intercalation into the interlayer (or interlayer adsorption) of MoS_2 nanosheets, we considered two possible sites including I_1 and I_2 for the 2H phase (see Fig. S2(a)) and three potential sites (I_1, I_2, and I_3) for the 1T phase (see Fig. S2(b)). The stability of Li adsorption and intercalation configurations is evaluated by calculating their binding energies E_b as follows,

$$E_b = E_{tot} - E_{MoS2} - E_{Li} \quad (1)$$

where E_{tot}, E_{MoS2}, and E_{Li} are the energies of adsorption system, pristine MoS_2 nanosheet, and Li atom, respectively. The binding energies and the corresponding configurations are listed in Table S1. For the surface adsorption, the Li adsorption at the H site has the biggest binding energies for both 2H and 1T phases, suggesting the highest stability for the Li adsorption at the site. For the interlayer adsorption, I_1 is the most stable adsorption site for the Li intercalation into 2H and 1T MoS_2 nanosheets, respectively.

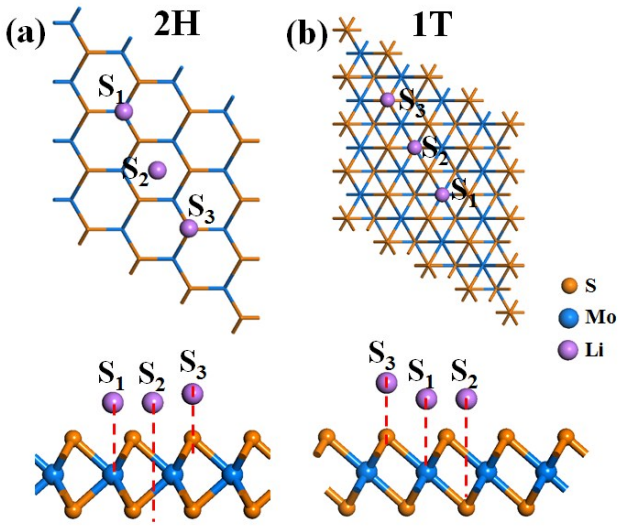

Fig. S1. Top and side views of possible surface adsorption sites of single Li ion on (a) 2H phase and (b) 1T phase MoS_2 nanosheets. S_x (x =1, 2, 3) denotes surface adsorption sites. The orange, blue, and purple balls represent S, Mo, and Li atoms, respectively.

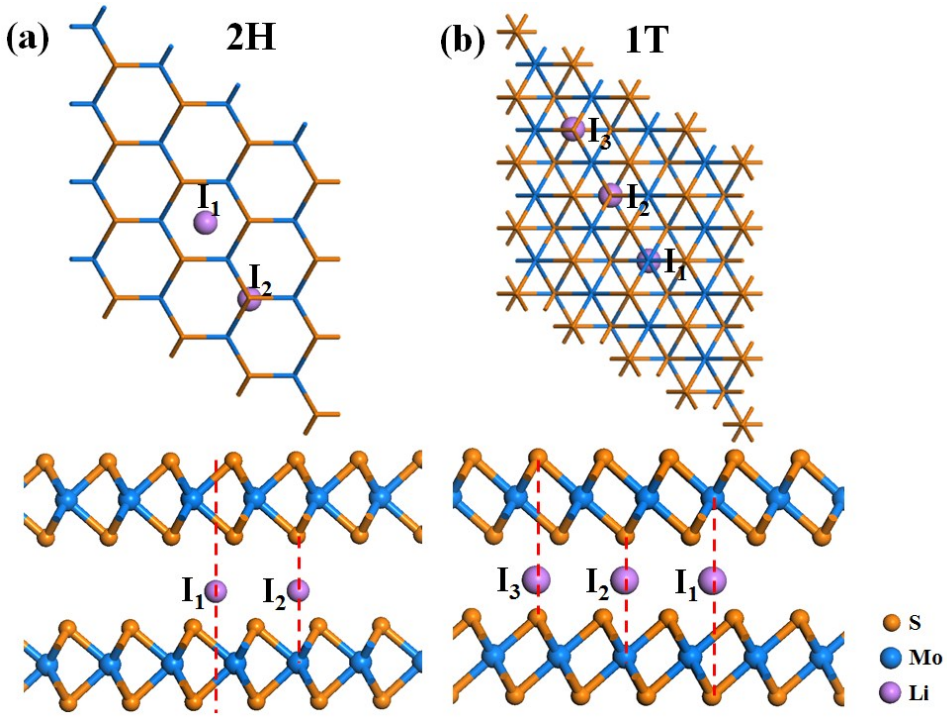

Fig. S2. Top and side views of possible interlayer adsorption sites of single Li ion on (a) 2H phase and (b) 1T phase MoS_2 nanosheets. I_x (x =1, 2, 3) denotes interlayer adsorption sites. The orange, blue, and purple balls represent S, Mo, and Li atoms, respectively.

Table S1. Potential sites and binding energies (in eV) of single Li ion adsorption/intercalation on 2H- and 1T-phase MoS_2 nanosheets.

Phase	Adsorption site	Binding energy (eV)
2H	**S_1**	**1.98**
	S_2	1.82
	S_3	1.27
1T	**S_1**	**4.22**
	S_2	4.16
	S_3	3.22
2H	**I_1**	**2.83**
	I_2	2.59
1T	**I_1**	**4.50**
	I_2	4.19
	I_3	4.02

II. Details of thermodynamic diagram calculations

In the thermodynamic equilibrium condition, the formation of Li-Mo-S ternary phases requires that the chemical potential of Li, Mo and S satisfy the following condition,[1,2]

$$x\Delta\mu_{\mathrm{Li}} + y\Delta\mu_{\mathrm{Mo}} + 2y\Delta\mu_{\mathrm{S}} = \Delta H(\mathrm{Li}_x\mathrm{Mo}_y\mathrm{S}_{2y}) \quad (1)$$

where $\Delta H(\mathrm{Li}_x\mathrm{Mo}_y\mathrm{S}_{2y})$ is the formation enthalpies of $\mathrm{Li}_x\mathrm{Mo}_y\mathrm{S}_{2y}$ ternary phase which are listed in Table S2. The atomic structures of $\mathrm{Li}_x\mathrm{Mo}_y\mathrm{S}_{2y}$ ternary phase are shown in Figure S3. The formation enthalpies are calculated by the following formula,

$$\Delta H(\mathrm{Li}_x\mathrm{Mo}_y\mathrm{S}_{2y}) = \mathrm{E}_{\mathrm{tot}} - x\mu_{\mathrm{Li}} - y\mu_{\mathrm{Mo}} - 2y\mu_{\mathrm{S}} \quad (2)$$

where $\mathrm{E}_{\mathrm{tot}}$ is the total energy of a $\mathrm{Li}_x\mathrm{Mo}_y\mathrm{S}_{2y}$ ternary phase, and μ_{Li}, μ_{Mo}, and μ_{S} are chemical potential of Li, Mo, and S elements which refer to the energies of their bulks. Here the values of x and y depend on the layer number n of nanosheets. We list the values of x and y and formation entropies of $\mathrm{Li}_x\mathrm{Mo}_y\mathrm{S}_{2y}$ with different layer numbers in Table S2. In order to avoid the formation of secondary $\mathrm{Li_2S}$ and $\mathrm{MoS_2}$ phase as well as the formation of Li, S and Mo bulk phase, the chemical potential also obey the following constraints,

$$2\Delta\mu_{\mathrm{Li}} + \Delta\mu_{\mathrm{S}} \le \Delta H(\mathrm{Li_2S}) \quad (3)$$

$$\Delta\mu_{\mathrm{Mo}} + 2\Delta\mu_{\mathrm{S}} \le \Delta H(\mathrm{MoS_2}) \quad (4)$$

$$\Delta\mu_{\mathrm{Li}} \le 0, \Delta\mu_{\mathrm{Mo}} \le 0, \Delta\mu_{\mathrm{S}} \le 0 \quad (5)$$

where $\Delta H(\mathrm{Li_2S})$ and $\Delta H(\mathrm{MoS_2})$ are the formation enthalpies of $\mathrm{Li_2S}$ and $\mathrm{MoS_2}$, respectively. The computed formation entropies of $\mathrm{Li_2S}$ and $\mathrm{MoS_2}$ are -4.07 eV and -2.64 eV. Using the eq.(1)-(4), the thermodynamic phase diagrams of lithiated $\mathrm{MoS_2}$ nanosheets can be obtained.

Table S2. The formula factors (x and y) and formation enthalpies (in eV) of 2H and 1T $\mathrm{Li}x\mathrm{Mo}y\mathrm{S}_{2y}$ ternary structures with different layer numbers.

Layer number n	x	y	$\Delta H_{2\mathrm{H}}(\mathrm{Li}_x\mathrm{Mo}_y\mathrm{S}_{2y})$	$\Delta H_{1\mathrm{T}}(\mathrm{Li}_x\mathrm{Mo}_y\mathrm{S}_{2y})$
1	2	1	-3.68	-4.08
2	3	2	-7.97	-8.82
3	4	3	-12.24	-13.57
4	5	4	-16.63	-18.30
∞	1	1	-4.29	-4.41

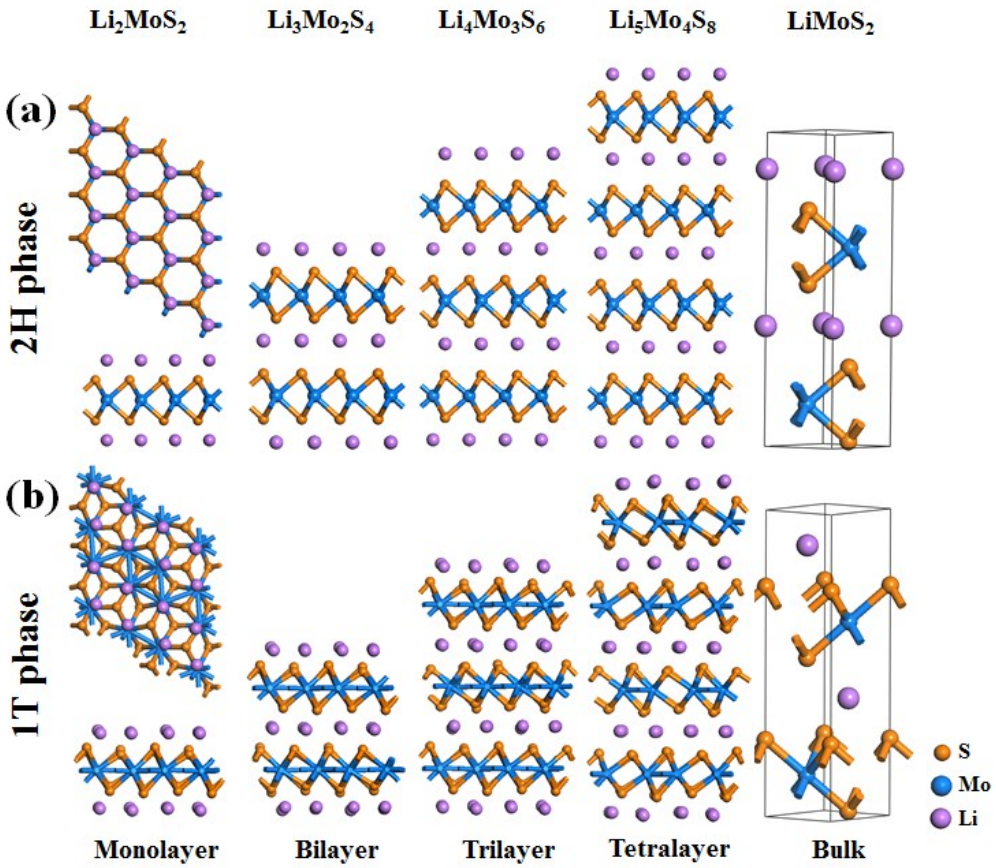

Fig. S3. Atomic structures of ternary $Li_xMo_yS_{2y}$ nanosheets and bulk in their (a) 2H phase and (b) 1T phase. Here both top and side views of monolayer atomic structure have been indicated, but only the side-view atomic structures are shown for other nanosheets due to their similar surface structures as indicated in the monolayer. The orange, blue, and purple balls represent S, Mo, and Li atoms, respectively.

III. Schematic illustration for the structural evolution of MoS_2 nanosheets in the cycling charge process

The Li intercalation causes the structural destruction of MoS_2 nanosheets, and the cycling discharge process induces the dissociation of MoS_2 sheets. This process follows a layer-by-layer dissociation mechanism, as shown in Fig. S5. The dissociated MoS_2 will participant in the formation of SEI film.

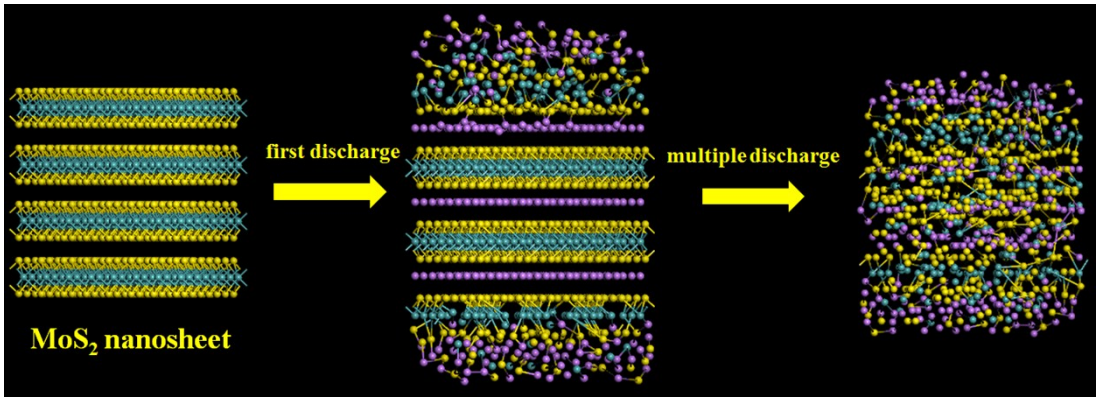

Fig. S4. Schematic illustration for the structural evolution of MoS_2 nanosheets in the discharge processes.

IV. AIMD trajectories for lithiated silicene/MoS_2/silicene composite

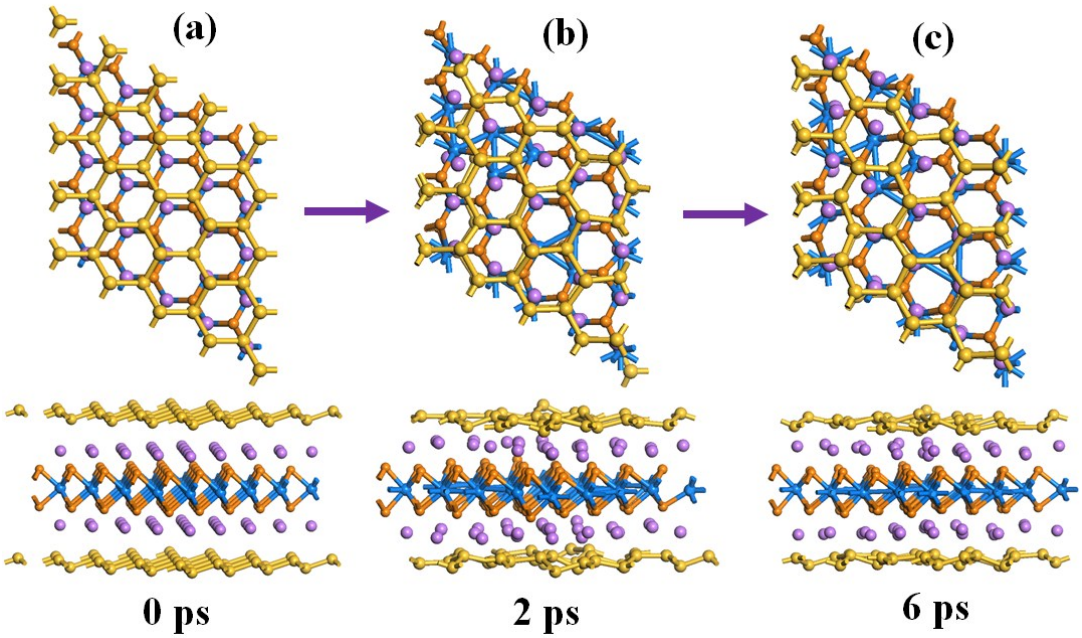

Fig. S5. Snapshots of trajectories for lithiated silicene/MoS_2/silicene composite structure following 6 ps AIMD simulation at 300 K. The yellow, purple, blue, and orange balls represent Si, Li, Mo, and S atoms, respectively.

V. Movies for recording the AIMD simulation results

Movie S1: The movie records the trajectories for the lithiated 2H-MoS_2 monolayer at 300 K within 6 ps.

Movie S2: The movie records the trajectories for the lithiated 1T-MoS_2 monolayer at 300 K within 6 ps.

Movie S3: The movie records the trajectories for the lithiated 2H-MoS_2/graphene composite structure at 300 K within 6 ps.